SLAC-PUB-337
September 1967

A 30-cm BORE 70-kG SUPERCONDUCTING HELMHOLTZ MAGNET*

by

H. Brechna and W. Haldemann
Stanford Linear Accelerator Center
Stanford University, Stanford, California

and

A. D. McInturff,[†] Atomics International

ABSTRACT

The design and performance of a 30-cm bore, 70-kG central field supermagnet with an axial gap of 8 cm will be described in detail. Preparatory work, such as choice of suitable hard superconductors and adequate substrates in combination with appropriate cooling, development of suitable insulations, current optimization, and the determination of size and number of modules in the coil, was necessary to venture in building a 5.2 Mj superconducting magnet. Studies on stability, field and force distribution and field homogeneity are presented. Four coil modules have been operated several times and their cool-down, current charging characteristics and operational performance will be given.

(Presented at 1967 Cryogenic Engineering Conference, Stanford University, August 21-23, 1967)

*Work supported by the U. S. Atomic Energy Commission

[†]Present address, Brookhaven National Laboratory

SUMMARY

This paper summarizes the design, procurement and testing of a 30-cm Helmholtz coil with a central field of 70 kG. In 1966 it was decided to build a large-scale supermagnet, which could be used for high energy physics experiments, as well as to be utilized as a general purpose magnet to study high field properties of new Type II superconductors, heat transfer, thermal conductivity, etc. The coils have an outer diameter of 90 cm and a total axial length of 66 cm with an axial gap of 8 cm. To utilize the full capability of the magnet, each coil half is subdivided into three modules which may be energized from one or separate current sources. When the inner coil alone is energized, the central field of 30 kG in stable mode is obtained; however, this section can be operated up to 35 kG without quench. The field homogeneity in the center is measured to be $\frac{\Delta B}{B} = 7 \times 10^{-4}$ inside a 2.0-cm diameter sphere and will be improved by adding higher-order solenoids inside the bore to achieve an homogeneity value of $\frac{\Delta B}{B} = 10^{-5}$ or 0.7 gauss.

The magnet has a stored energy of 4.8 Mj and a weight of 1600 kg. It is energized by means of battery banks which are charged simultaneously in continuous mode. The various superconducting cables were acquired from commercial companies, but the design work, building of coil forms, support structures and the 4-m high, 1.2-m diameter dewar were accomplished at SLAC.

The continuous supply of liquid helium during operation is provided by a 7-watt liquefier, which delivers 11 liters of liquid helium per hour. The helium gas, which evaporated due to heat radiation, thermal conduction, and heating of the current leads, is stored in four large high-pressure tanks, and is repurified and reliquefied for further use in a closed circuit process. The present SLAC system can store about 1000 liters of liquid helium and 100 m^3 of gaseous helium

at 8.6 kg cm^{-2}. It is estimated that the loss of helium per month through the system is about 20 percent.

The first three cool-downs were performed by means of liquid nitrogen to 78° K, pressure reduction inside the dewar to 70° K and cool-down to 4.2° K with liquid helium.

The weight of the magnet components, excluding support structures, are given in Table I.

TABLE I

WEIGHT OF MAGNET COMPONENTS

Inner coils	112.5 kg	Superconductor	162 kg Cu
Middle coils	18 kg	Superconductor	225 kg Cu
Outer coil	67.5 kg	Superconductor	427 kg Cu
Stainless steel parts and flanges	324 kg		
Aluminum flanges, etc.	135 kg		
Miscellaneous parts	100 kg		

Total energy required to cool down four inner modules was 5.2×10^6 Ws; for the total coil, 8.4×10^6 Ws.

Using the enthalpy of gaseous helium, which passes through the coil, and assuming about 40 percent cooling efficiency of the system (measured), the four modules could be cooled with 330 liters of liquid helium and the whole coil with 535 liters of liquid helium.

The conditions in the laboratory required that the liquifier is located approximately 12 meters from the main dewar. However, using the cool-down scheme shown in Fig. 1 and using the liquifier as a refrigerator (power output at 20° K ~ 200 watts) we were able to cool down the magnet and dewar system to 20° K and then down to 4.2° K with liquid helium from separate dewars. Under this condition the total amount of liquid helium required was 30 liters for four inner modules including flanges and support structure, and 50 liters for the total coil.

Attempts to cool down the magnet to 4.2°K using the liquifier were unsuccessful. For immersing the coil totally in liquid helium, approximately 400 liters were necessary. The coil was operated for several hours and, due to partial quenches, about 300 liters of liquid helium evaporated. From the total amount of 1400 liters available liquid helium, about 70 percent was recovered in gaseous form.

Four modules operated from two separate current sources have produced until now 45 kG. Several reasons explained below were responsible for the fact that the design field of 50 kG was not reached at the first operations.

At a second test the total coil was energized to 64.2 kG where a first quench due to instability of the intermediate coil occurred. It is estimated that ~ 350 liters of helium were evaporated within 10 seconds. The coil was again operated and with the exception of minor trouble, no major damage in the coil was encountered.

Rearranging mode of charging the coil will produce more than 70 kG at the center.

PREPARATORY AND MODEL WORK

Building a superconducting magnet, which in size and field can be used for high energy experiments, presents problems which have to be faced and resolved, prior to final decision of size, material and configuration. Safety of operation and the fact that the magnet may be used for experimental purposes and should be able to operate over thousands of hours dictate a careful and systematic study of winding configuration, selection of superconducting materials to be used, grading of the superconductor, coil division into appropriate modules, insulation materials, stress distribution and cooling efficiency.

Theoretically, after basic magnet features are specified, such as central transverse field, field homogeneity in the gap in a certain volume, and stability of operation, the basic coil geometry and the average current density over the coil can be determined. Lines of constant field can be plotted which yield the optimum distribution of At. However, from a practical point of view, the calculated At distribution over the coil cannot always be met due to conductor and insulation tolerances, and thus the first calculation is an approximation. The performance of the stabilized cable is lightly degraded due to handling, and if the magnet cooling is not adequate or controlled over the entire coil, the upper limit of the coil current may be less than the design value.

The conductor and layer insulation have to withstand thermal shocks, mechanical stresses and fatigue due to repeated cycling. Mechanical rigidity is important to prevent interturn shorts and conductor movements and guarantee the hydraulic diameter of helium passages.

In order to determine actual winding distribution, space factors, and cooling efficiency, several small-size model coils with bore diameters ranging between 3 - 7 cm, axial length 10 - 25 cm and outer coil diameter 10 - 20 cm with different conductor shapes, various insulation configurations, geometry and composition, were built and tested.

From several insulation materials tested at 300° K and 77° K as shown in Table II, a polyamid braid with the dimensions 0.05×0.130 cm (under compression) was selected, which was wrapped in a helical form around individual conductors, with 1.72 turns per cm length of conductor.

Prior to coil winding, the attempt was made to form the composite superconductor and copper cable to a square shape; however, only a small coil was wound and tested in the laboratory. Manufacturing problems prevented obtaining square cables carrying a current of 500 A at 80 kG commercially. The conductor used in our magnet is a cylindrically-shaped composite cable of superconductors and copper strands as illustrated in Fig. 2.

Due to the rectangular cross section of the insulation braid and its tolerances, the theoretically assumed triangular winding configuration could not be achieved, and thus the calculated space factors did not agree with the actual magnet.

Calculated and measured current densities, as well as central flux density values for the magnet, are shown in Table III.

In order to obtain a compactly wound coil, the wire tensions during winding had to be kept at certain values over the coil. To find the correlation between wire tension and superconductor degradation; tensile tests with Ti (22 at % Nb) were performed, which are illustrated in Fig. 3. After each tensile test, the stress was reduced to its initial value of 0.25 kg cm^{-2} and the current-carrying capacity at constant transverse fields measured. The permanent degradation limit due to stress was determined when the current density of the conductor at 0.25 kg cm^{-2} tensile stress deviated from the original value prior to the tensile experiment. For our particular application, a cable tension of 35 - 50 kg cm^{-2} was chosen, which was kept constant over each coil module by means of winding and tension devices shown in Fig. 4.

The distribution and size of the various coil modules, given in Table I, were due to a number of reasons:

1. Each coil pair can be energized separately and used as an independent entity, thus giving three magnets with various $\int B d\ell$ for specific experiments, or connected in series as desired.
2. The radial, axial and tangential stresses on the conductor and the compressive strength on the insulation can be limited to values which do not exceed insulation compressive strength. Fatigue strength of the insulation is higher than predicted compressive stresses due to magnetic forces. Wire movements can be prevented. Short circuits between turns and layers are eliminated or localized.
3. The length of radial cooling channels between individual conductors are kept short and thus the heat transfer between conductor and bulk coolant is enhanced.

The modules can be slipped radially on each other. The set of six modules is bolted between 3-cm thick stainless steel and aluminum flanges for mechanical rigidity.

The superconductor for the various sections was chosen as follows:

1. Inner Section: Radial distribution of the axial field at the conductor is 75 - 45 kG. The 0.35-cm diameter stabilized cable consisted of superconductor Ti (22 at % Nb); substrate certified OFHC copper, annealed (Fig. 2-I). The superconductors are graded according to the H-J characteristic of the conductor and the field distribution over the inner module. The number of superconductors in the cable is changed gradually in radial direction from six to three, and replaced by copper conductors. The short sample characteristic and the H-J curves of various tested superconductors and cables are illustrated in Fig. 5. The copper resistance per unit length of the copper substrate as a function of temperature and field is given by the relation:

$$R_{m;4.2°K} = R_{0;293°K}\left[\frac{0.9}{\frac{R_{0;293°K}}{R_{0;4.2°K}}} + 0.25 \cdot B_m \cdot 10^{-2}\right] \quad \text{(ohms)} \qquad (1)$$

   The cable is impregnated with a 7% Ag-Sn alloy for rigidity and better heat conduction, as well as an improvement in mechanical strength (7% Ag-Sn alloy has a tensile strength of 1140 - 1400 $kg \cdot cm^{-2}$).

2. Middle Section: Radial distribution of axial field is 43 - 25 kG; the 0.264-cm diameter stabilized cable consisted of superconductor Ti (22 at % Nb); substrate certified OFHC copper, annealed (Fig. 2-II). The central superconductor is graded according to the best short sample and cage test performance (Fig. 6) and is unchanged dimensionally. The section with

poorer H-I performance is placed at the low field radial section of the module.

3. Outer Section: Maximum field at the conductor is 23 - 30 kG; the 0.36-cm diameter stabilized cable consists of Nb(48%)Ti and Nb(25%)Zr; substrate, certified OFHC copper, annealed. (Fig. 2-III)

It was decided to use liquid helium pool boiling, where the coil is immersed in liquid helium. The coil, with a total weight of 1600 kg, is attached to a vacuum vessel and is bolted to the dewar flange as shown schematically in Fig. 7.

COIL INDUCTANCE AND CHARGING TIME

If the coil is wound and insulated such that no interturn or interlayer shorts occur, the coil inductance is given by:

$$L = \sum_{i=1}^{n} L_i + 2 \sum_{\substack{i \neq j \\ i=1 \\ j=1}}^{n,m} M_{i,j} \tag{2}$$

The section self-inductance L_i and the mutual inductance M_{ij} may be obtained from literature.[1,2] The so-called magnet charging time is dictated by the terminal voltage of the current source. However, if internal shorts appear in the magnet, the charging time is prolonged due to the reduction of the shunt resistance and the change of L. The current flows in a complicated $L_m - R_m$ network inside the magnet. In order to study the effect of internal shorts between turns or layers, a series of small magnets mentioned above was wound and tested. Results are summarized in Table IV.

Thus it seems imperative in large volume magnets to eliminate any kind of short-circuited turns and layers in order to reduce charging time or change the central field according to the experimental need within reasonable limits. This, of course, is governed by L of the system and the terminal voltage.

For our magnet, calculated self-inductance is

$$\sum_{1}^{6} L_i = 12 \text{ Hy} \quad ;$$

mutual inductances

$$\sum M_{ij} = 10 \text{ Hy} \quad ;$$

and the total coil inductance,

$$L = 32 \text{ Hy} \quad .$$

With an operating current of I = 500 A and having all turns in series, the coil energy is $E = 4.0 \times 10^6$ joules. However, if the magnet is operated from several power supplies, the energy of the coil is 5.2×10^6 joules. The calculated charging time T_c = 1200 sec for a terminal voltage of 12 volts.

COOLING AND STABILITY

It is evident that besides using low electrical resistivity metals in combination with superconductors, cooling and improvement of thermal capacity of the coil play equally important roles in the stability of superconducting coils. Even though copper or aluminum substrates provide a parallel low resistance current passage when the transition from superconducting to normal state occurs, it has been shown[3,4] that poorly cooled coils have a greater tendency to degrade. The use of normal low resistance substrates in an open-wound coil with adequate cooling improves the thermal capacity of the system and leads to a more stable performance, at current values comparable to short sample tests. Steady state stability criteria for pool boiling indicate that improvement in heat transfer yields a reduction in the amount of shunt-normal material in combination with the superconductor. Thus, the overall space factor is improved, yielding higher average current densities.

If pertinent precautions are neglected, the open-wound structure may become mechanically weak. Thus, the introduction of appropriate insulation and reinforcing, which prevents macroscopic conductor movements, are necessary.

From various winding techniques currently being used, layer-wound techniques were chosen, where the insulation braid was wrapped in helical form around the conductor. Only 70 percent of the conductor area is exposed to the coolant. Radial and axial cooling gaps provided by the 0.05 cm thick insulation braid eliminated interturn shorts. The correct choice of insulation thickness, width, and number of helical turns per unit length of conductor is a function of the conductor size and coil geometry; however, its lower thickness limit is given by the heat transfer coefficient of liquid helium. Cooling channels of less than 0.015 cm are not recommended, in order to prevent trapping of helium bubbles which would lead to hot spots.

The first attempts to use a high resistance square strip (Manganin, Constantan) with suitable thermoset-coated surfaces failed due to microscopic insulation abrasion at the edges of the strip. The insulation control of the high resistance metallic helix over the entire length of the strip ($\sim$ 22,500 meters) was practically impossible. Monofilament organic insulations and glass epoxy filaments did not withstand repeated cycling between room and cryogenic temperatures and thus were discarded. A multifilament polyamid, heat-treated braid was finally selected due to its desirable performance.

The influence of adequate cooling in achieving stable coil performance and still obtaining current densities in the order of 5×10^3 Acm^{-2} with transverse fields of 7 - 8 Vs/m^2 at the conductor was previously emphasized. Three main reasons are given below:

1. Improvement in thermal capacity of the superconducting system.
2. Enhancement of heat transfer.
3. Uniformity of temperature over the entire coil.

This last reason is of specific interest for Nb_3Zr and $Nb_{2-3}Ti$ alloys and their ternaries.

From conductor geometries seen in Fig. 2, the steady state heat transfer coefficients calculated and measured for stable operation are given in Table III.

Further increase of current above the stable limit drives portions of the superconductor normal and thus a fraction of the total current flows through the substrate.

To investigate the limit of stable operation, a simplified analysis of the thermal characteristics is given below:

We consider a portion of the inner coil section with the highest transverse field and refer to the cable geometry in Fig. 2-I. The cable diameter is 0.35 cm, the coolant gap w = 0.046 cm (min.) and the length of an axial coolant flange between turns $z \cong 0.35$ cm. Assume this portion of the superconductor is normal and the design current of 500 A does flow through the copper substrate. The critical power density may be calculated from the correlation equation by Sydoriac, Roberts[5] and Wilson.[6]

$$p_c = \frac{w}{\sqrt{z}} \cdot \frac{L\,d_\ell}{2} \cdot \left[\frac{q \cdot g}{\beta - 1}\left(1 - \frac{\ln\left[1 + q(\beta - 1)\right]}{q(\beta - 1)}\right)\right]^{\frac{1}{2}} \left(W\ cm^{-2}\right) \quad (3)$$

with

L = latent heat of the boiling liquid (Wsg^{-1})

g = 981 cm sec^{-2} (earth acceleration)

d_ℓ = liquid density

$\beta = \frac{d_\ell}{d_v}$ = ratio of liquid to vapor density

q = quality factor assumed 0.35, corresponding to the short gap length

For our particular geometry the critical power density is $p_c = 0.51$ W cm^{-2} per unit length of the conductor.

At the design current of I = 520 A, the power density per unit cooling surface (~30% covered by insulation) is 0.316 W cm^{-2}, indicating nucleate helium boiling. The comparison to p_c indicates that the coil may be able to operate to a limit of 625 A. However, due to the complex coil matrix a safety factor was more advisable. It should also be pointed out that we did not exceed in any of our magnets of a similar structure the value of $p = 0.4$ W cm^{-2}.

COIL STRUCTURE AND STRESS DISTRIBUTION

The determination of the axial and radial forces leads to the corresponding σ_r, σ_c, and σ_a stress distribution in the coil. As the general theory of forces would be beyond the scope of this paper, we will give pertinent results and refer to literature.[7] In Figs. 8-a and 8-b, the axial and radial field distribution of the coil are illustrated. For uniform current distribution throughout each module, the forces on each conductor may be calculated. Forces F_a and F_r in the median plane yield the stresses σ_r, σ_c, and σ_a. By using failure theory, we may locate the element where failure will occur in the coil.

Using the field distribution, the tangential stress at the composite cable was calculated to be 1000 kg$\cdot$ cm^{-2}, the radial stress 175 kg$\cdot$ cm^{-2} and the axial stress 380 kg$\cdot$ cm^{-2} maximum. The combined axial and radial stress on the cable results in a compressive stress of 6.5×10^3 kg$\cdot$ cm^{-2}, on the helical multifilament insulation. The insulation withstands this stress, as can be seen from strength data after repeated cycling given in Table II. Each module is additionally wrapped in a unidirectional glass-polyester and stainless steel tape, for reinforcement. The conductor itself is not reinforced.

COIL PERFORMANCE AND TESTS

The four inner coil modules were energized by two current stabilized dc power supplies independently and simultaneously. The two inner modules (I in Fig. 2) showed an upper stable current limit of 525 A, corresponding to 29.5 kG, the modules of the intermediate section (II in Fig. 2) 507 A, corresponding to 17 kG. Both coils energized simultaneously could be energized to 505 A, corresponding to 45 kG. The current voltage oscillograms are shown in Fig. 9. The coil was charged to the maximum field in less than 20 minutes. The experiment was discontinued due to excessive helium boiling, which made recovery of gaseous helium impossible (Fig. 10).

A later check-up, to find why the four modules did not reach 50 kG or more, revealed the following:

a. The cable used in the intermediate section has one central superconductor. Thus the conductor is sensitive to flux jumping. If the magnet is charged fast, the heat generated in the superconductor cannot be removed adequately.

b. The superconductor exhibits a considerable amount of training, which is seen from oscillogram in Fig. 11 and the magnetization curves, Fig. 12. The correlation of the flux jumps from the two tests are in good agreement. After three cycles the coil does not show any appreciable training. However, so much helium was boiled off during the first tests that the experiment had to be discontinued.

c. The joints from superconductor to copper lead had shown signs of erosion, and thus the joint resistance was increased one order of magnitude, heating up the turns adjacent to the leads.

d. Several external turns of the intermediate module had become loose during operation which resulted due to a better coil packing and thus were sensitive to current sweep.

It is realized by now that even if the Nb, Ti superconductor does not exhibit size effects up to 0.1-cm diameter conductor, it becomes rather unstable and sensitive to current and flux sweep. Current charging became more delicate, and the module must be charged rather slowly to prevent extensive helium boiling.

Several of the above deficiencies have been corrected in the meantime, with the exception of the cable in the intermediate section, which primarily will dictate the charging speed of the magnet.

After all 6 modules were wound, the coil was energized as follows: Outer section (III) to 503 Amp, inner section (I) to 455 Amp and middle section (II) to 353 Amp. The measured field at the center was 64.2 kG corresponding to field energy of $\sim 4 \cdot 10^6$ joules (Fig. 13). Due to the unstable behavior of the superconductor in the middle section, a quench occurred at 353 Amp which resulted in the evaporation of $\sim$ 350 liters of helium within 10 seconds.

Successively the two coil sections (III) and (I) were energized to 600 Amp and 500 Amp, respectively, without difficulties, which showed that the coil had passed a quench at 4 mega-joules without major damage. The middle section of the coil will be replaced and it is certain that a field of $\sim$ 70 kG can be reached with the coil.

REFERENCES

1. E. B. Rosa and F. W. Grover, "Formulas and Tables for the Calculation of Mutual and Self Inductance," N.B.S. Paper 169.
2. H. Brechna, "A High Field 1.3 m Superconducting Split Coil Magnet with Forced Liquid Helium Cooling," presented at Superconductivity Conference, Zurich, May 1966.
3. R. D. Cumings and W. N. Lathan, "An Experimental Measurement of Dependance of the H-I Curve of NbZr Wire in Temperature," J. Appl. Phys. 36, 2971 (1965).
4. R. Hancox, "Stability Against Flux Jumping in Sintered Nb_3-Sn," Phys. Letters 16, 208 (1965).
5. S. G. Sydoriak and H. R. Roberts, "Study of Boiling in Short Narrow Channels and its Application to Design of Magnets Cooled by Liquid H_2 and N_2," J. Appl. Phys. 28, 143 (1957).
6. M. N. Wilson, "Heat Transfer to Boiling Liquid Helium in Narrow Vertical Channels," Rutherford Laboratory, Preprint of Paper II-2, June 1966.
7. L. M. Lontai and P. G. Marston, "A 100 kG Quasi-Continuous Cryogenic Solenoid," Part I, Proc. Intl. Symposium on Magnet Technology CONF - 650922, 1965, Clearing House for Federal Scientific and Technical Information, National Bureau of Standards, U. S. Dept. of Commerce, Springfield, Virginia 22151.

TABLE II

PHYSICAL PROPERTIES OF MULTIFILAMENT TAPES AT 300°K AND 78°K [1]

PROPERTIES	INSULATION TAPE: Glassfibre Impregnated[2] Epoxy	Glassfibre Impregnated[2] Silicone	Polyester Monofilament	Polyamid[3] Heat Treat.	Polyamid[3] Silicone Impr.
Tensile Strength (kg. cm^{-2})	$3 \cdot 10^4$		$1.1 \cdot 10^3$	$4 \cdot 10^3$ (2% elongation)	
Breaking elongation (%)	< 1		11	∼8	
Initial Modulus (kg. cm^{-2})	$8 \cdot 10^5$		$7 \cdot 10^4$	$2.5 \cdot 10^5$	
Compressive Strength (kg. cm^{-2})	$2 \cdot 10^4$	$2.6 \cdot 10^4$	$(3.5 \ldots 7) \cdot 10^3$	$(0.6 \ldots 1.2) \cdot 10^4$	
Thermal Conductivity ($W . cm^{-1} . {}^{\circ}K^{-1}$)	$3 \cdot 10^{-3}$		$1.2 \cdot 10^{-3}$	$1.1 \cdot 10^{-3}$	
Specific Gravity (g. cm^{-3})	2.55		1.1-1.4	1.3	
Specific Heat ($Ws . g . {}^{\circ}K^{-1}$)	0.4		0.6	0.7	

- - - - - - - - - - - - - -

1.) Average of 5 samples. Strength values ± 30%.

2.) Very brittle. Fracture during wrapping and repeated cycling.

3.) Also called Nomex Nylon. Dupont trade name.

TABLE III

CALCULATED AND MEASURED SLAC SUPERMAGNET PARAMETERS[1)]

	CALCULATED	MEASURED[5)]
N_{inside}	5,000	4,140
N_{middle}	2,800	2,400
$N_{outside}$	5,200	4,140
I_{stable}[2)] (Amp)	510	400
λJ_{stable}[2)] ($Amp.cm^{-2}$)	$4.15 \cdot 10^3$	10^3
I_{stable}[3)] (Amp)	500/505/550	455/353/503[6)]
λJ_{stable}[3)] ($Amp.cm^{-2}$)	$4.3 \cdot 10^3$	$3.4 \cdot 10^3$
$B_{o,o}$[2)] (T)	7.2	5.7
$B_{o,o}$[3)] (T)	7.8	6.42
B_c[4)] (T)	7.7[2)]; 8.4[3)]	7.0
I_{max}[2)] (Amp)	525	400
I_{max}[3)] (Amp)	525/540/600	500/355/600
T_{charge} (Sec.) (12V power supply)	1,200	10,000
Time Const. (Sec.) (Coil shunted)	~ 500	2,000
E Coil[2)] (joules)	$3.8 \cdot 10^6$	$2.6 \cdot 10^6$
E Coil[3)] (joules)	$5.2 \cdot 10^6$	$4 \cdot 10^6$
$h\Delta T$ (inside) (Wcm^{-2})	0.35	0.24
$h\Delta T$ (middle) (Wcm^{-2})	0.34	0.125
$h\Delta T$[3)] (outside) (Wcm^{-2})	0.2	0.144

----

1) Coil dimension may be obtained from Figure 7.

2) All modules in series.

3) Modules energized from three current sources

4) Max. transverse field at conductor.

5) First full operations.

6) Inner and outer sections (I, III) not fully energized.

TABLE IV

MODEL TESTS

Coil N°	I	II	III	IV	V	VI (HELMHOLTZ COIL) (IV AND V)
a_1(cm)	1.35	3.85	3.55	3.51	3.65	3.51; 3.65
α	2.2	2.42	2.74	2.7	2.45	2.7; 2.45
β	1.88	2.42	2.5	2.66	2.56	2.66; 2.56 2g = 4.76 cm
N	375	735	854	688	728	1,416
Number Layers	12	16	16	16	16	16
Cond. Composition (Cable)	Square: 6 Nb,Zr 13 Cu (0.03 cm ϕ)	Zylindric 7 Nb,Zr 54 Cu (0.03 cm ϕ)	as II	as II	as II	as II
Insulation	Nichrome, bare (0.012 x 0.038) cm^2	Nichrome, thermoset coated, (0.045 x 0.076) cm^2 many shorts.	No interturn insulation 0.08 cm Phenolic Spacer between layers	Glass fibre braid (0.081 x 0.2) cm^2	Nomex[3]) braid (0.04 x 0.19) cm^2	as IV, V
I Stable (Amp)	300	760	675	775	720	690
I Quench (Amp)	540	780	700	790	735	700
I Recovery (Amp)	200	710	600	715	680	
λJ Stable ($Amp.cm^{-2}$)	1.33×10^4	5.72×10^3	5.27×10^3	4.8×10^3	5.3×10^3	4.48×10^3
$B_{(o,o)}$ (T)	3.85	3.1	3.2	2.95	2.90	1.97
Coil Weight (kg)	1.13	25	27.2	24.5	25.6	50.1
$h\Delta T$ ($W.cm^{-2}$)	0.4	0.376	0.295	0.39	0.34	0.31

LIST OF FIGURE CAPTIONS

1. SLAC Magnet Refrigeration System

2. 70-kG, 30-cm bore superconducting magnet

3. Current carrying capacity vs applied mechanical tension. Parameter: transverse field

4. Outer coil section during winding. At left: Tension device and monitoring system

5. Short sample characteristics of various superconductors, Type II.

   1. Nb_3Sn (RCA)
   2. Nb (25%) Zr (Supercon)
   3. Ti(22 at % Nb) old wire (AI)
   4. Nb (48%) Ti, old conductor (Supercon)
   5. Nb (48% Ti) (Supercon)
   6. Nb (48%) Ti cable (Supercon)
   7. Ti (22 at % Nb) (AI)

6. Superconducting cable and cage

7. 30-cm coil assembly and dewar

8a. Axial field components

8b. Radial field components

9. Terminal voltage and current oscillograms

   1. Inner coil section
   2. Intermediate coil section

10. Coil after completion of the first experiment

11. Voltage current oscillograms of a 5-cm bore, 10-cm long coil, 38-kG, wound with AI cable illustrated in Fig. 2-II.

    1...3 Three successive runs

12. Magnetization curves of the AI conductor shown in Fig. 2-II

    1. First run. 2. Second run.

13. Voltage and current oscillograms of the 30-cm coil. The 3 sections have been energized simultaneously by means of 3 power supplies.

Top: Inner section

Middle: Intermediate section

Bottom: Outer section

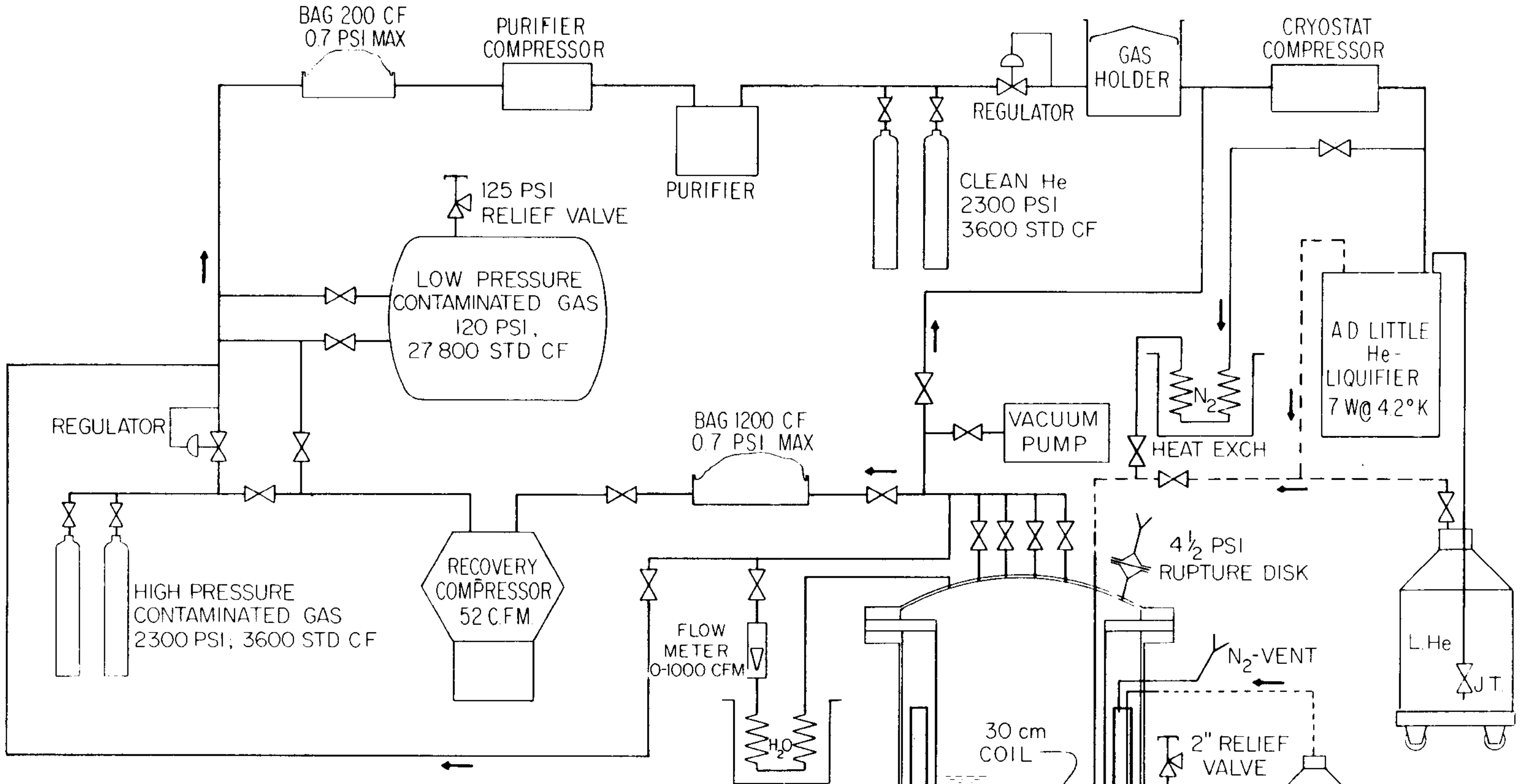
BAG 200 CF
0.7 PSI MAX
PURIFIER
COMPRESSOR
PURIFIER
REGULATOR
GAS
HOLDER
CRYOSTAT
COMPRESSOR
CLEAN He
2300 PSI
3600 STD CF
125 PSI
RELIEF VALVE
LOW PRESSURE
CONTAMINATED GAS
120 PSI,
27 800 STD CF
A.D. LITTLE
He-
LIQUIFIER
7 W@ 4.2°K
N2
HEAT EXCH
VACUUM
PUMP
REGULATOR
BAG 1200 CF
0.7 PSI MAX
4½ PSI
RUPTURE DISK
HIGH PRESSURE
CONTAMINATED GAS
2300 PSI; 3600 STD CF
RECOVERY
COMPRESSOR
52 C.F.M.
FLOW
METER
0-1000 CFM
H2O
N2-VENT
L.He
J.T.
30 cm
COIL
2" RELIEF
VALVE

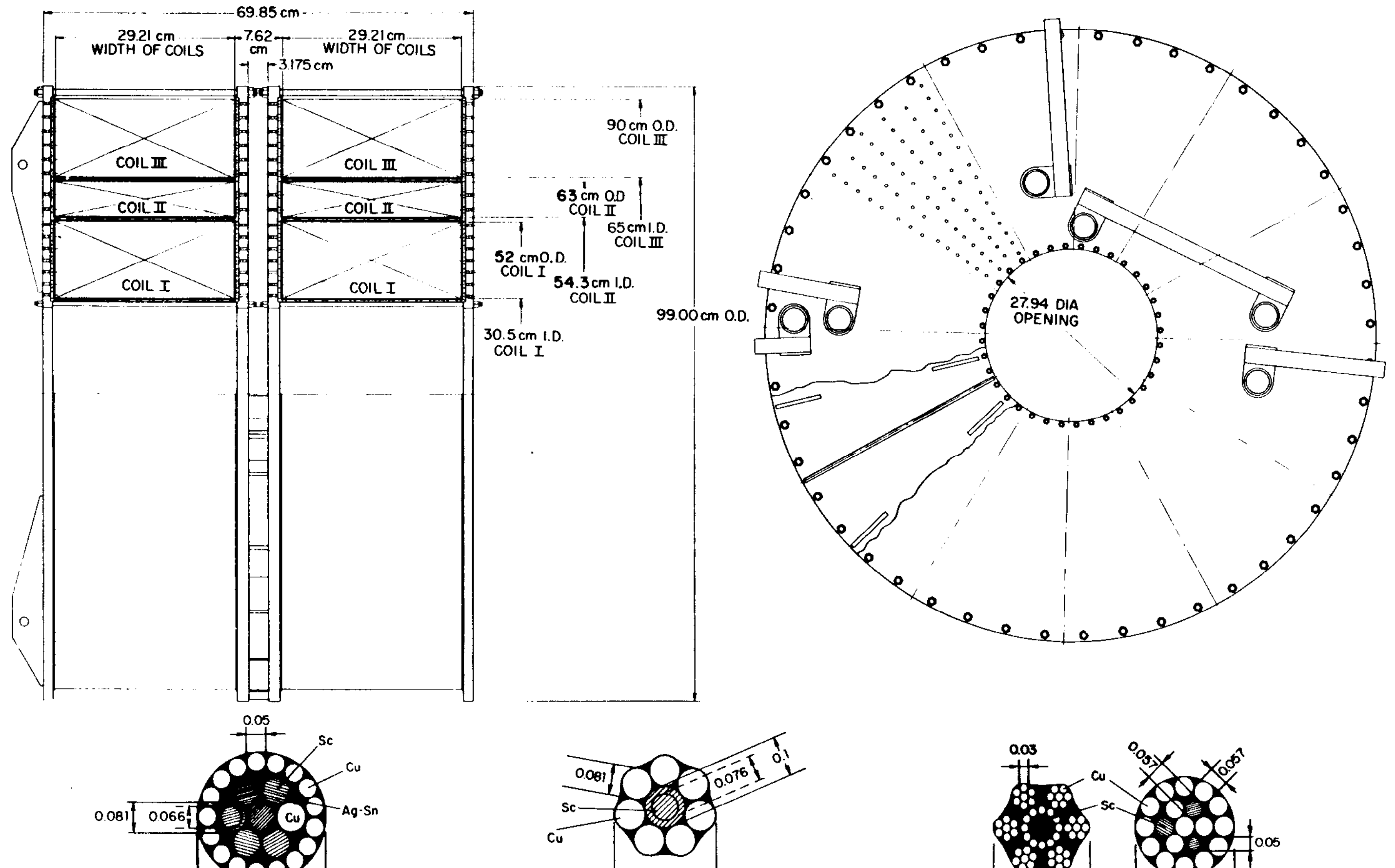
69.85 cm
29.21 cm WIDTH OF COILS
7.62 cm
3.175 cm
29.21 cm WIDTH OF COILS
COIL III
COIL II
COIL I
90 cm O.D. COIL III
63 cm O.D COIL II
65 cm I.D. COIL III
52 cm O.D. COIL I
54.3 cm I.D. COIL II
30.5 cm I.D. COIL I
99.00 cm O.D.
27.94 DIA OPENING
0.05
Sc
Cu
Ag-Sn
0.081
0.066
0.076
0.1
0.03
0.057

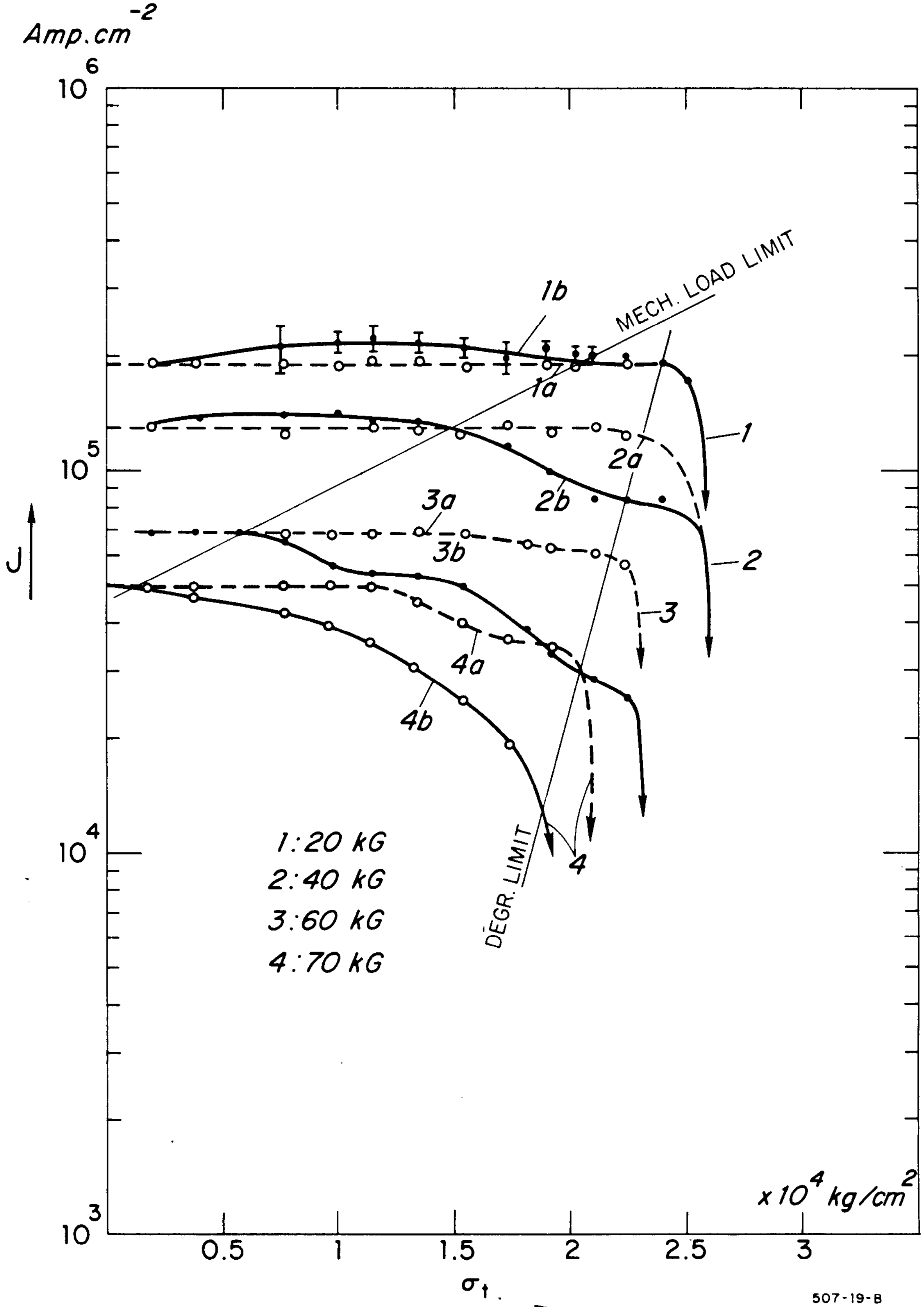

Amp.cm^{-2}
10^6
10^5
10^4
10^3
J
1b
1a
MECH. LOAD LIMIT
1
2a
2b
2
3a
3b
3
4a
4b
4
DEGR. LIMIT
1: 20 kG
2: 40 kG
3: 60 kG
4: 70 kG
x 10^4 kg/cm^2
0.5
1
1.5
2
2.5
3
σ_t
507-19-B

Fig. 3

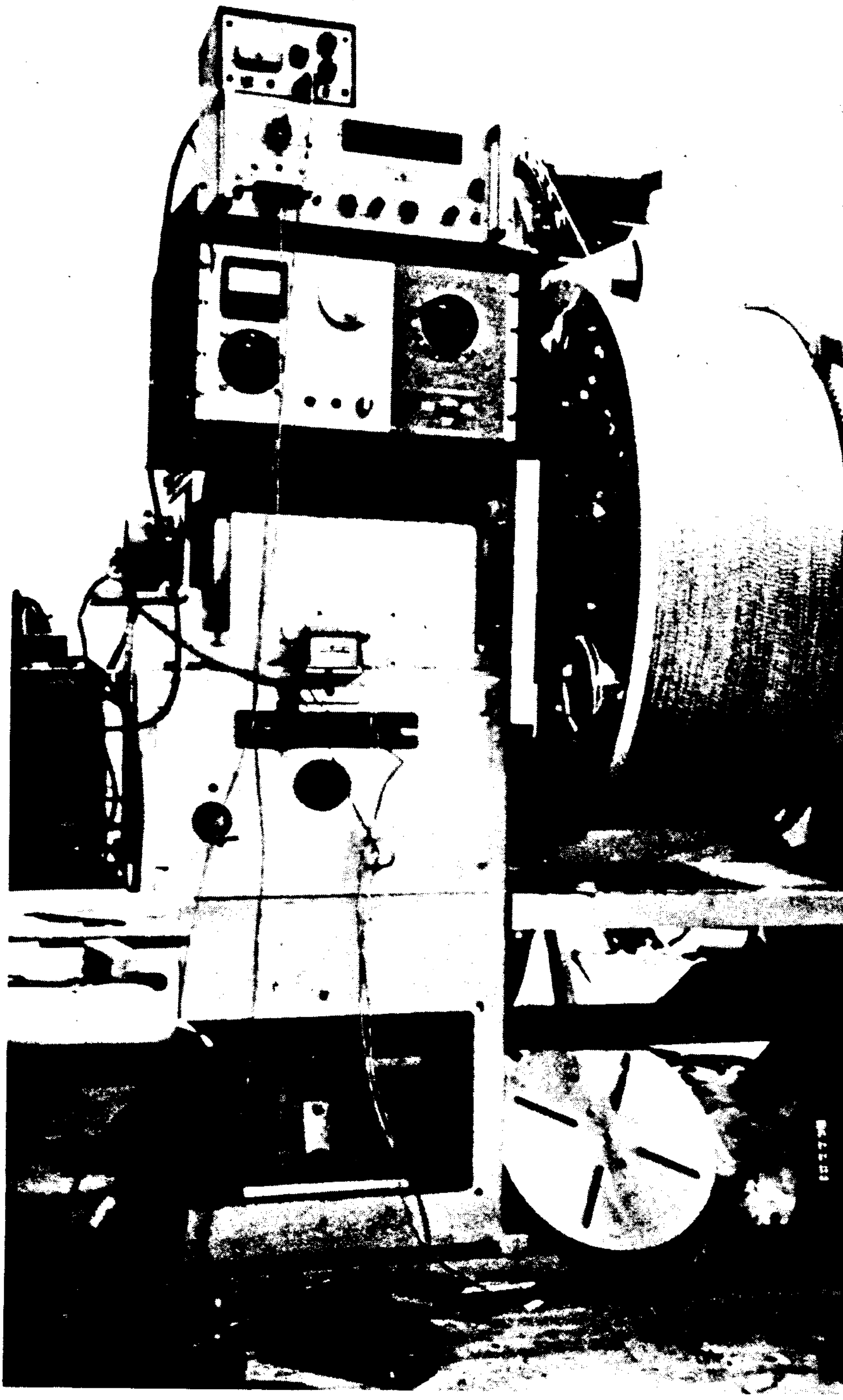

Fig. 4

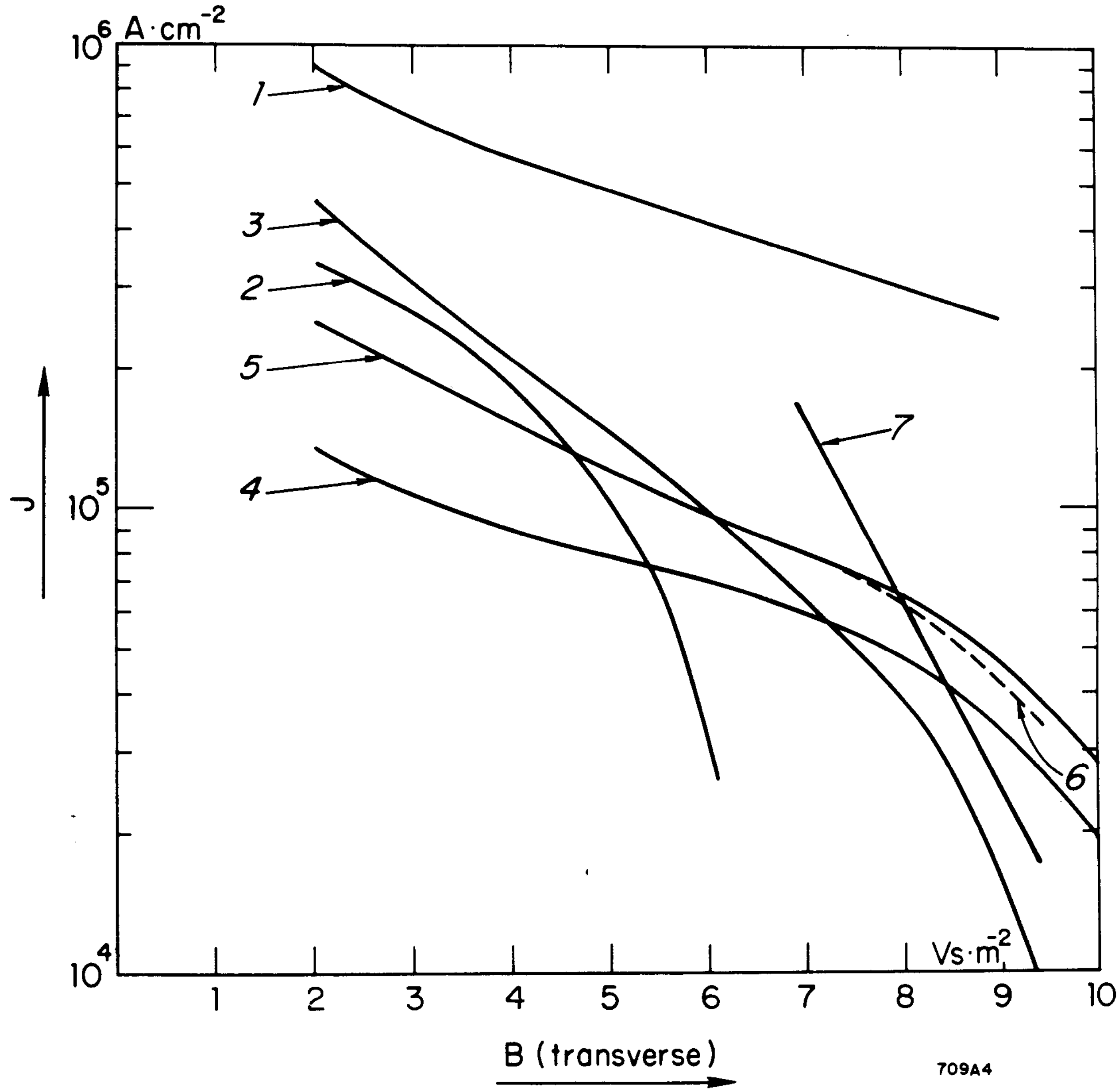
10^6 A·cm^-2
10^5
10^4
J
1
2
3
4
5
6
7
Vs·m^-2
1
2
3
4
5
6
7
8
9
10
B (transverse)
709A4

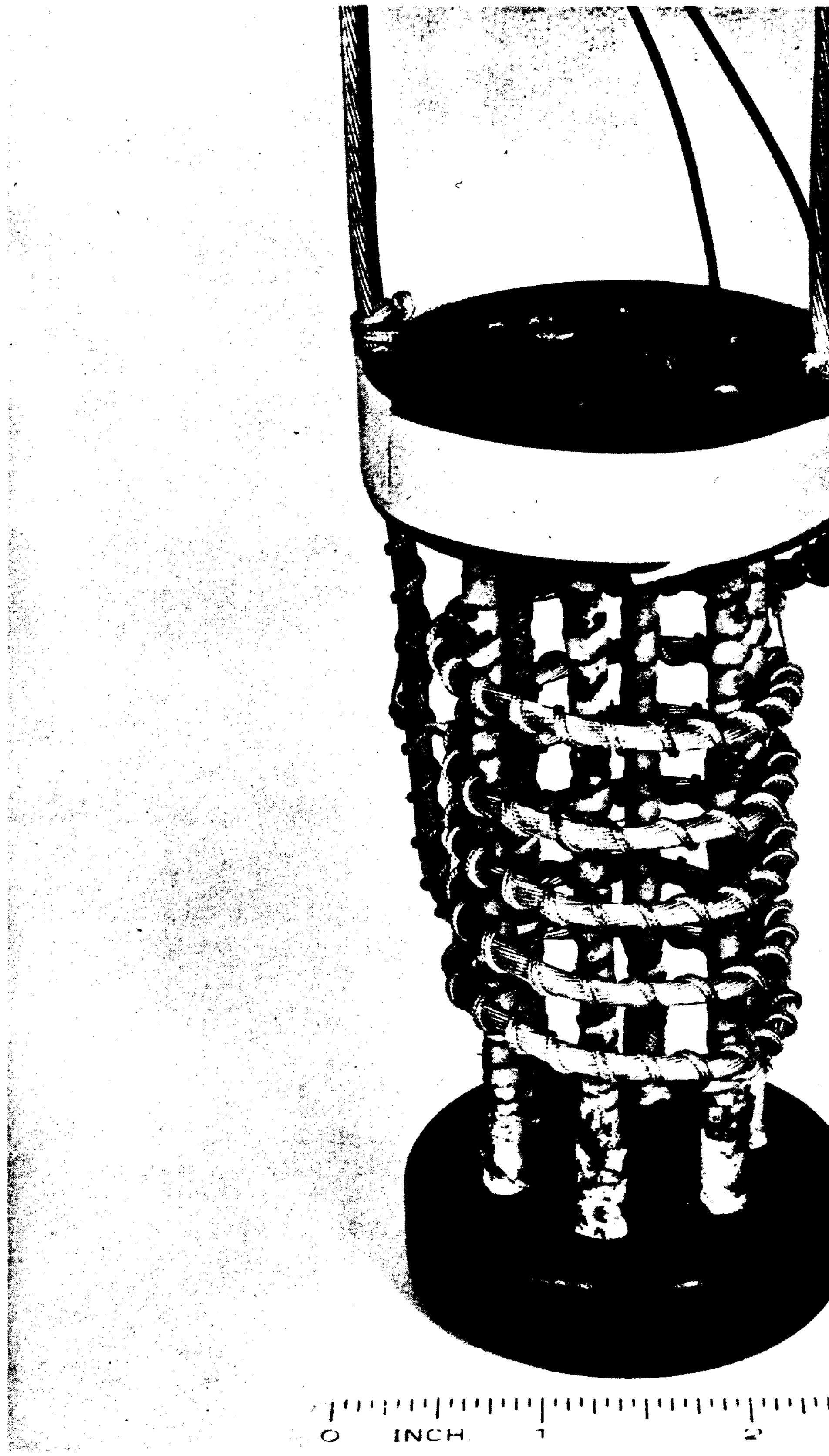

Fig. 6

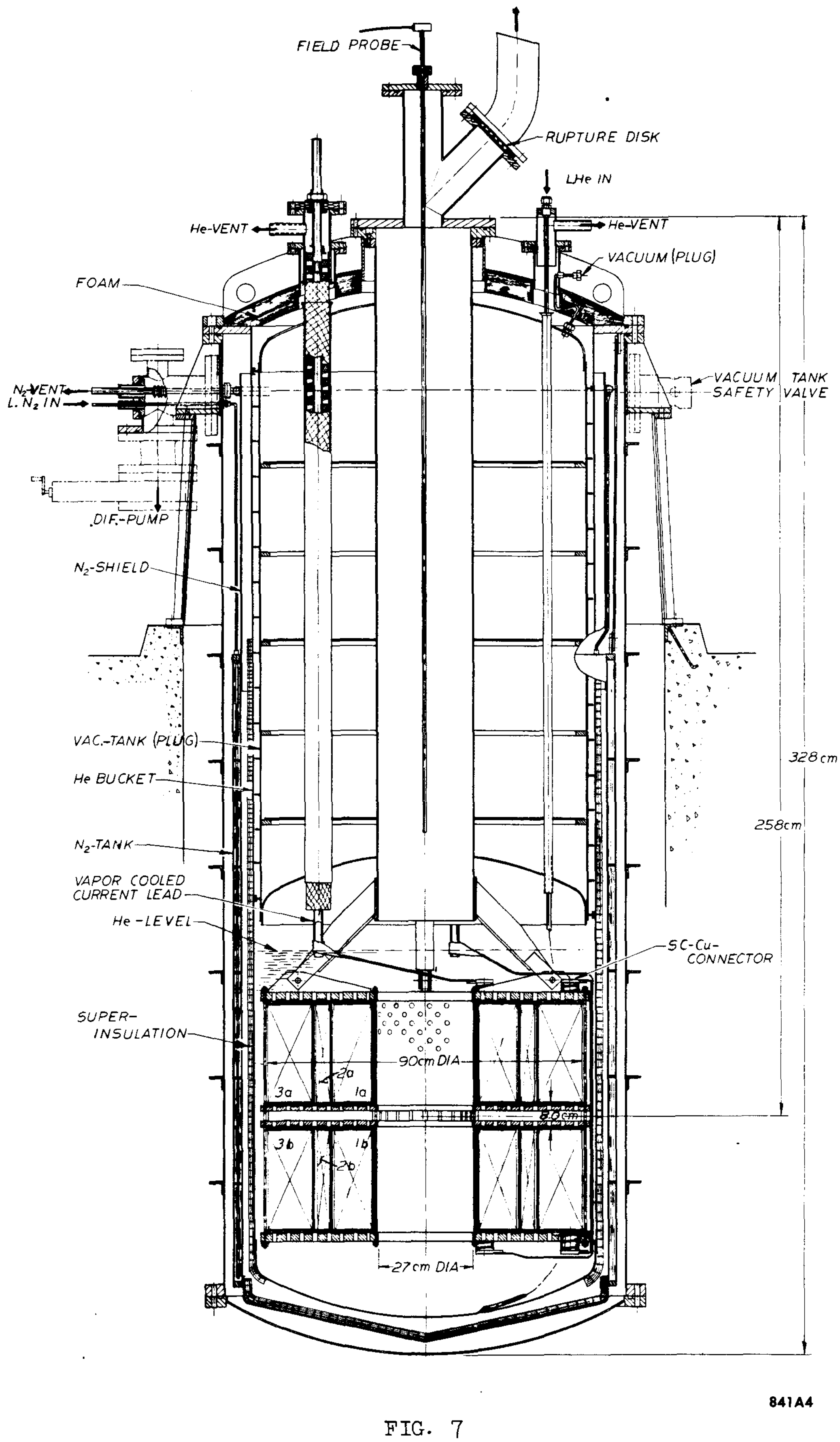

FIELD PROBE
RUPTURE DISK
LHe IN
He-VENT
He-VENT
VACUUM (PLUG)
FOAM
N2-VENT
L. N2 IN
VACUUM TANK
SAFETY VALVE
DIF.-PUMP
N2-SHIELD
VAC.-TANK (PLUG)
He BUCKET
N2-TANK
VAPOR COOLED
CURRENT LEAD
He-LEVEL
SC-Cu-
CONNECTOR
SUPER-
INSULATION
328 cm
258 cm
90 cm DIA
8.0 cm
3a
2a
1a
3b
1b
2b
27 cm DIA
841A4

FIG. 7

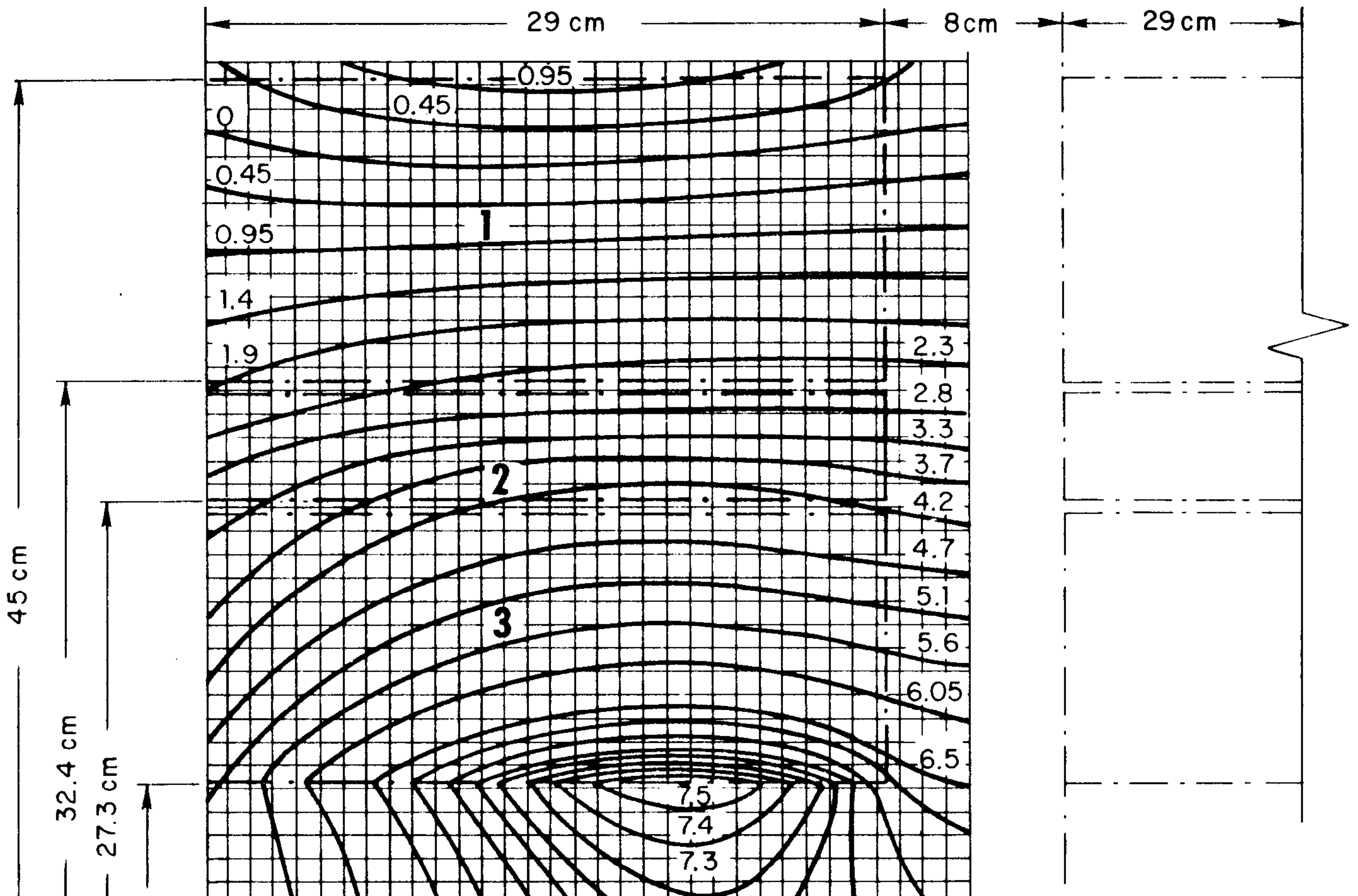

29 cm
8cm
29cm
45 cm
32.4 cm
27.3 cm
0.95
0.45
0
0.45
0.95
1.4
1.9
1
2
3
2.3
2.8
3.3
3.7
4.2
4.7
5.1
5.6
6.05
6.5
7.5
7.4
7.3

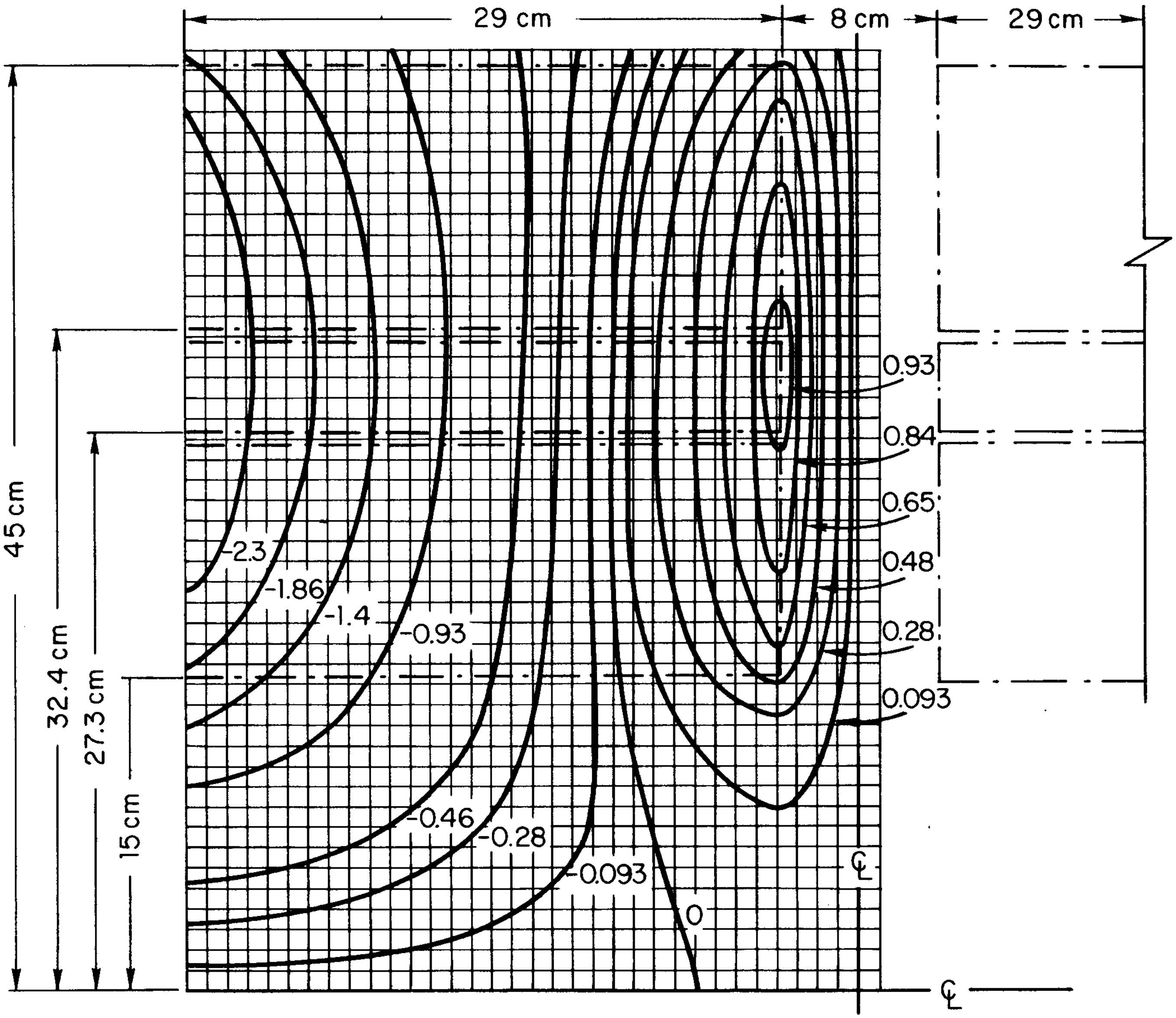

FIG. 8b

841A12

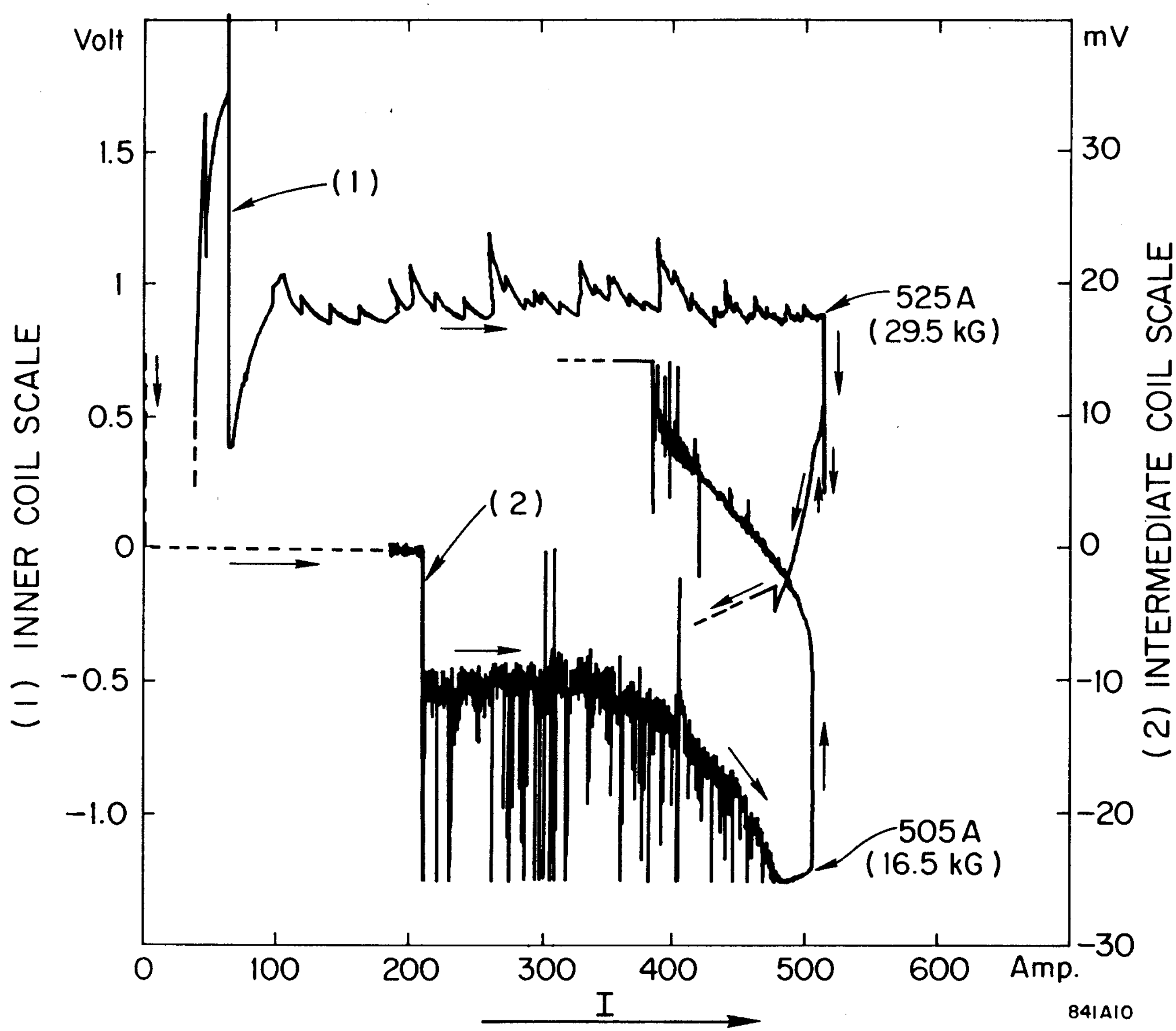
Volt
mV
1.5
1
0.5
0
-0.5
-1.0
30
20
10
0
-10
-20
-30
(1) INNER COIL SCALE
(2) INTERMEDIATE COIL SCALE
(1)
(2)
525 A
(29.5 kG)
505 A
(16.5 kG)
0
100
200
300
400
500
600
Amp.
I
841A10

Fig. 9

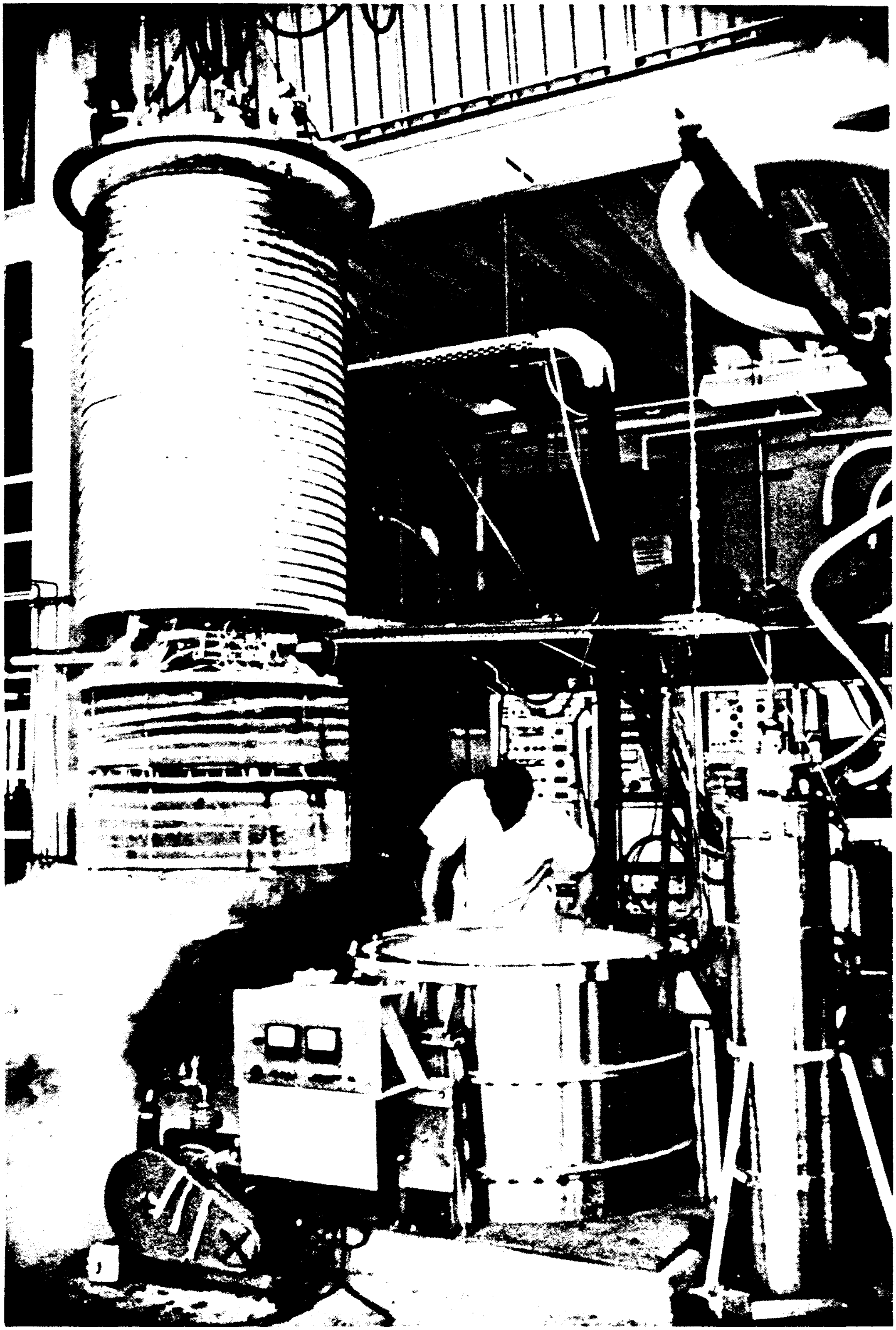

Fig. 10

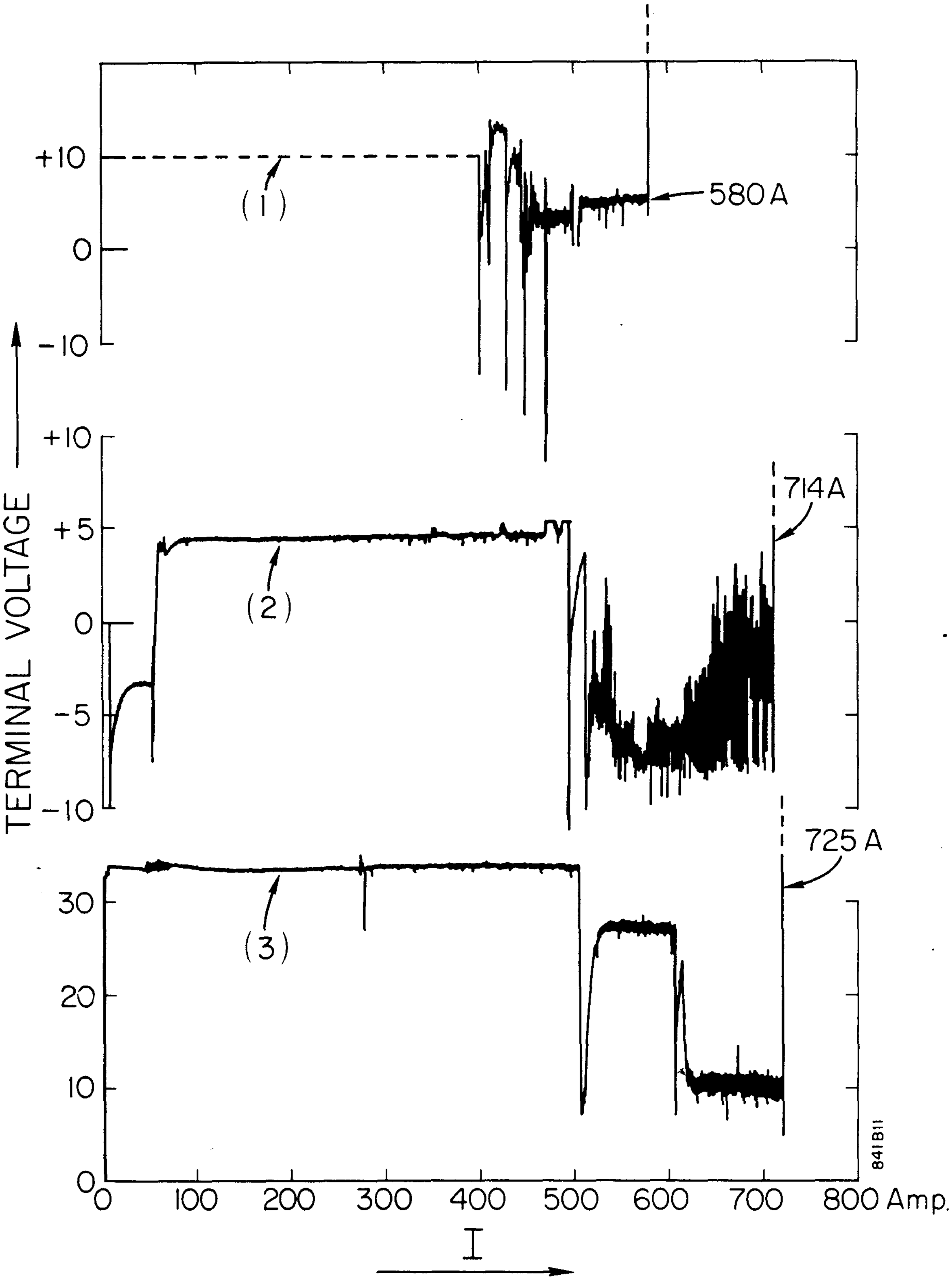
+10
(1)
580 A
0
-10
+10
+5
714 A
(2)
0
-5
-10
TERMINAL VOLTAGE
725 A
30
(3)
20
10
0
0
100
200
300
400
500
600
700
800 Amp.
I
841B11

FIG. 11

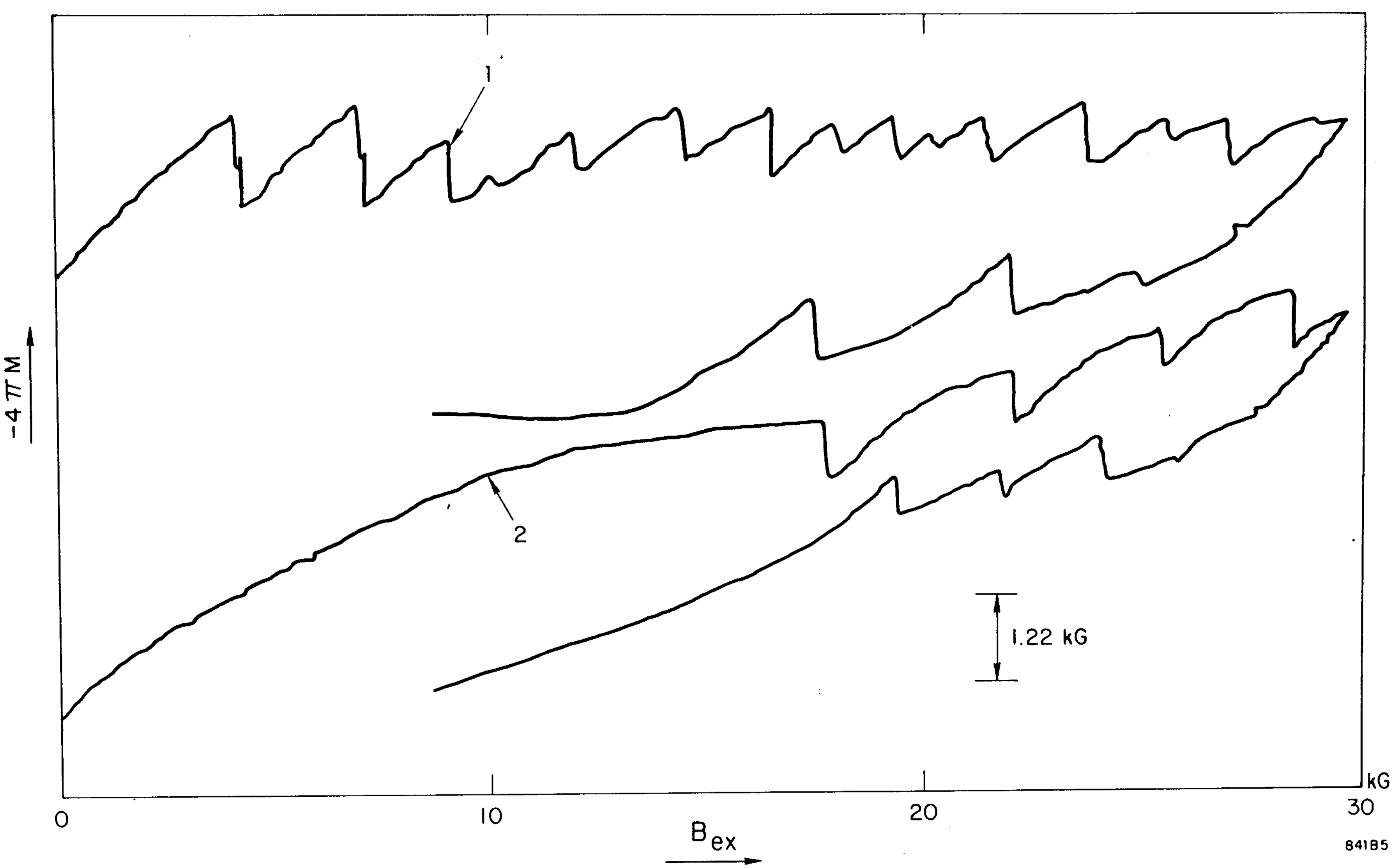

Fig. 12

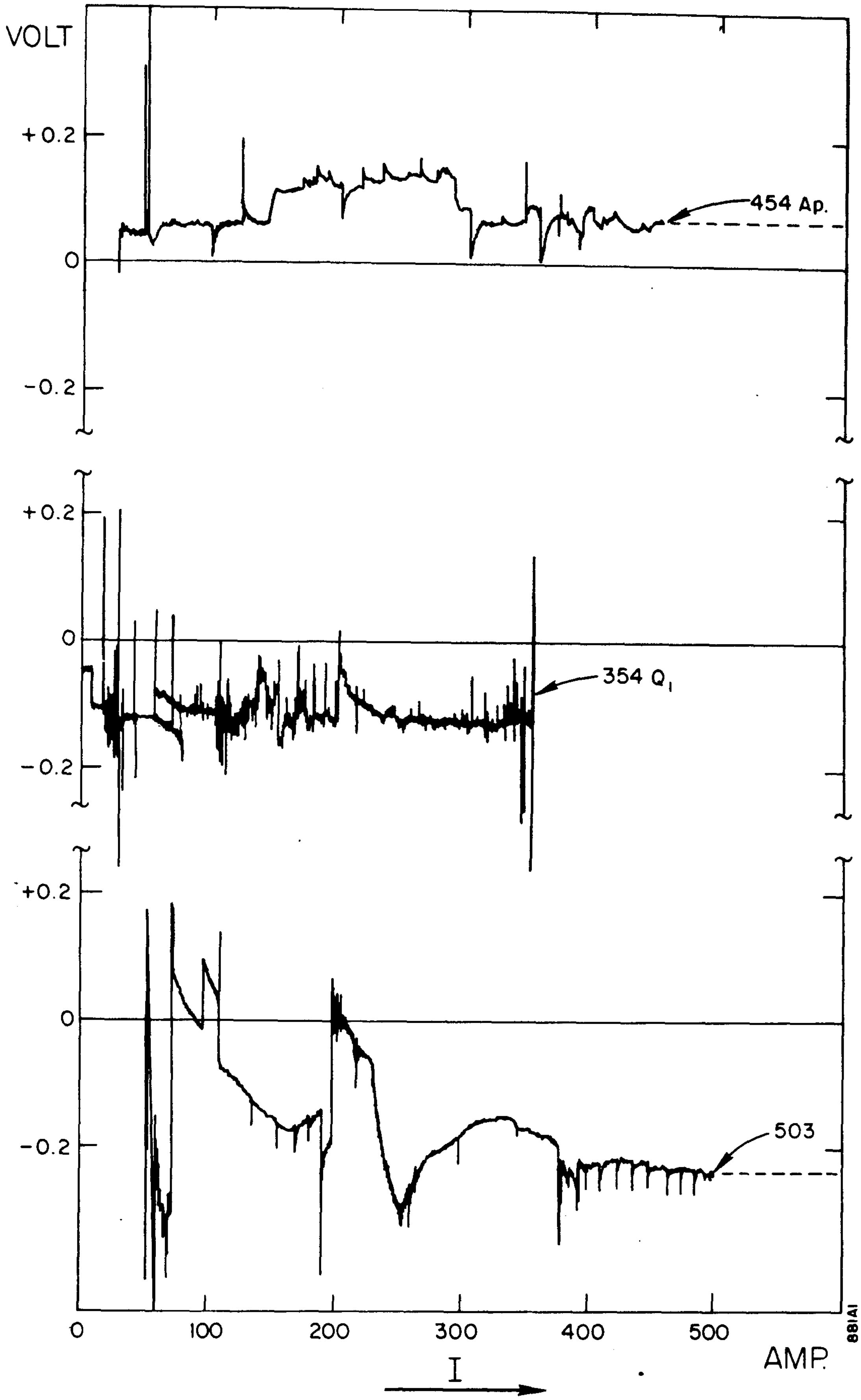
VOLT
+0.2
0
-0.2
454 Ap.
+0.2
0
-0.2
354 Q_1
+0.2
0
-0.2
503
0
100
200
300
400
500
AMP.
I
881A1

Fig. 13